

Myocardial Infarction

Hemorrhagic Myocardial Infarction After Coronary Reperfusion Detected *In Vivo* by Magnetic Resonance Imaging in Humans: Prevalence and Clinical Implications

Koichi Ochiai,¹ Toshio Shimada,¹ Yo Murakami,¹ Yutaka Ishibashi,¹ Kazuya Sano,¹ Jun Kitamura,¹ Shin-ichi Inoue,¹ Rinji Murakami,² Hideaki Kawamitsu,³ and Kazuro Sugimura³

¹Fourth Division, Department of Internal Medicine, Shimane Medical University, Izumo, Japan

²Emergency Unit, Shimane Medical University, Izumo, Japan

³Department of Radiology, Shimane Medical University, Izumo, Japan

ABSTRACT

With the advent of thrombolytic therapy, hemorrhagic myocardial infarction (HMI) has been observed in experimental and human autopsy studies. However, its clinical implications remain undetermined, because of the absence of a reliable method to detect its presence in vivo. This study was designed to evaluate the clinical implications of HMI detected by magnetic resonance (MR) imaging in vivo after coronary reperfusion. Thirty-nine patients with acute myocardial infarction (AMI) were studied. Percutaneous transluminal coronary angioplasty (PTCA) was used to reopen the occluded coronary artery. Electrocardiogram (ECG)-gated T2-weighted gradient-echo MR imaging was performed to detect intramyocardial hemorrhage, using a 1.5-T magnet within 2 weeks after coronary reperfusion (average, 5.7 days). Thirteen patients (33%) showed intramyocardial hemorrhage as a distinct hypointense zone by gradient-echo MR imaging and 26 patients showed homogeneous intensity consistent with absence of intramyocardial hemorrhage. Coronary angiograms showed lesser development of collateral flow in the patients with HMI than in those without (81% vs. 37%). Infarct size, estimated 1 month after coronary reperfusion by thallium-201 scintigraphy, was larger among patients with HMI than in those without ($37 \pm 14\%$ vs. $21 \pm 14\%$, respectively, $p < 0.05$). Left ventricular ejection fraction at 1 month follow-up showed less recovery in patients with HMI than in those without (47*

Received July 22, 1998; Accepted January 29, 1999

Address reprint requests to Toshio Shimada.

± 9 to $51 \pm 10\%$; $p = 0.47$, vs. 53 ± 10 to $60 \pm 9\%$, respectively, $p < 0.05$). ECG-gated T2*-weighted gradient-echo MR imaging offers a noninvasive means of detection of intramyocardial hemorrhage in patients with reperfused AMI. HMI occurred even after primary PTCA and may be a common finding associated with severely injured myocardium.

KEY WORDS: Acute myocardial infarction; Magnetic resonance imaging; Reperfusion.

INTRODUCTION

Recent animal studies have shown that intramyocardial hemorrhages are common in acutely reperfused myocardial infarction. During the clinical development of thrombolytic therapy, hemorrhagic myocardial infarction (HMI) was only noted at *postmortem* examination (1–6). Its clinical significance remains unclear, because of the lack of reliable methods to identify the presence of intramyocardial hemorrhage *in vivo*.

Magnetic resonance (MR) imaging is capable of detecting the presence of hemorrhage in tissue, for instance in patients with intracerebral hemorrhage (7–11). Red blood cell breakdown products such as deoxyhemoglobin, methemoglobin, or hemosiderin are paramagnetic and therefore generate static magnetic field inhomogeneities that reduce the localized signal intensity in T2-weighted spin-echo and gradient-echo MR imaging. These imaging techniques have been applied to myocardial tissue. Lotan et al. (12,13) showed the presence of intramyocardial hemorrhage in a canine model of acute myocardial infarction (AMI) using *ex vivo* T2-weighted spin-echo imaging. We previously reported intramyocardial hemorrhages detected by *in vivo* gradient-echo MR imaging in patients with anterior AMI (14). However, there are little published data on HMI in humans, and its prevalence and clinical significance after coronary reperfusion have not been examined in survivors of AMI.

In the present study, MR imaging with T2*-weighted gradient-echo sequence, a technique highly sensitive to broken down paramagnetic hemoglobin products, was used to detect intramyocardial hemorrhages in patients with reperfused myocardial infarction in an effort to define more precisely the prevalence and the clinical significance of HMI in humans. This study was performed after obtaining informed consent from the participants, in accordance with the ethical standards on human experimentation of our institution.

METHODS

Pilot Study of Autopsy Findings Versus MR Images

The pathologic findings at autopsy of a 65-year-old patient who died of intractable ventricular arrhythmias 3 days after coronary reperfusion were compared with MR imaging. The occluded proximal left anterior descending coronary artery had been recanalized with percutaneous transluminal coronary angioplasty (PTCA) 18 hr after the onset of chest pain. *Ex vivo* imaging was performed with medical instrumentation operating at 1.5 T (SIGNA, General Electric) with a head coil. T1-weighted spin-echo (TR = 500 ms; TE, 20 ms) and T2*-weighted gradient-echo (flip angle, 30 degrees; TR, 500 ms; TE, 25 ms) images were obtained *ex vivo*, 3 hr after the autopsy. Images were obtained using a multislice technique in short-axis planes perpendicular to the long axis of the heart with 8-mm slices, 2-mm gaps, two signal averages, a field of view of 24 cm, and an image matrix of 256×256 . The heart was sectioned similarly in 1-cm-thick slices, and the macroscopic findings were compared with the MR images.

Studies in Control Subjects Without Coronary Artery or Myocardial Disease

MR imaging was performed using the same instrumentation in 12 men and 8 women (mean age 63 ± 10 yr) who had no visible coronary artery disease or myocardial disease on angiography and echocardiography. Electrocardiogram (ECG)-gated gradient-echo imaging was used with a TR equal to one cardiac cycle, a TE of 25 ms, and a flip angle of 30 degrees to enhance T2*-based contrast, using body coils. Images were acquired using a multislice technique in planes perpendicular to the long axis of the heart with 8 mm in thickness, 1-mm gaps, two signal averages, a field of view of 32 cm, and an image matrix size of 192×256 . The images were

then displayed as a 512×512 matrix. The examination lasted an average of 15 min. Polyvinyl alcohol gel, of which relaxation times were known (T_1 , 272 ms; T_2 , 92.4 ms), was settled on the chest along the long axis of the heart as a reference of signal intensity. Measurement of signal intensity was carried out by selecting four regions of interest (1.0 cm^2) in the myocardium. The signal intensity ratio was calculated by dividing the average signal intensity of the myocardium by that of polyvinyl alcohol gel.

Studies in Patients with AMI

Patient Population

Thirty-nine patients (24 men and 15 women, mean age 65 ± 9 yr) with a first AMI due to single-vessel coronary artery disease were studied. A diagnosis of AMI was made on the basis of typical chest pain lasting more than 30 min, ST segment elevation in two or more leads of the standard 12-lead ECG, and an increase in serum creatine kinase (CK) above twice its normal level ($>300 \text{ IU/l}$). All patients underwent coronary angiography and left ventriculography on admission and 1 month later. Primary PTCA was performed in 36 patients whose initial coronary angiogram showed total vessel occlusion or a residual stenosis $> 90\%$ before PTCA. The other three patients showed spontaneous coronary reperfusion with thrombolysis in myocardial infarction (TIMI) flow grade 3 on initial angiogram, and coronary angioplasty was not performed. No patient received a thrombolytic agent, but all received oral aspirin (81 mg) and heparin, 5,000–10,000 units/day, after the first catheterization. Patients whose infarct-related coronary artery was reoccluded at angiographic reexamination 1 month later were excluded from the study. All patients were clinically stable while MR imaging was performed, and all medical therapy was continued during the study protocol.

MR Imaging in Patients with AMI

ECG-gated T_2^* -weighted gradient-echo MR imaging was performed in the acute stage (2–14 days after PTCA, mean 5.7 days) and the chronic stage (24–35 days after PTCA, mean 29 days), using the instrumentation and techniques described for the pilot and control studies. The images were visually and qualitatively analyzed by three independent observers. The presence of intramyocardial hemorrhage was inferred when images on more than two contiguous slices showed low signal intensity in the territory of the culprit coronary vessel. We settled polyvinyl alcohol gel on each patient's chest and measured signal

intensity of center of infarction (low signal intensity zone), its peripheral region, and remote region of myocardium.

Analysis of Coronary Angiograms and Left Ventriculography

The coronary angiograms were interpreted visually by two independent observers in a blinded fashion. TIMI and collateral flow grades were evaluated from the coronary angiogram before PTCA. Collateral flow in the 30 patients with TIMI flow grades < 2 was graded on a scale of 0–3, depending on the degree of opacification of the occluded vessel (15): 0, no collateral flow; 1, side branches of the perfused artery filled from collateral vessels; 2, epicardial segment partially filled from collateral vessels; 3, epicardial segment completely filled from collateral vessels. Collateral flow grades of 0 and 1 were considered poor, and collateral flow grades of 2 and 3 were considered good.

Left ventriculography was performed in the 30-degree right anterior oblique (RAO) position and the 60-degree left anterior oblique (LAO) position, using a power injector. Left ventricular ejection fraction was calculated using the area length method. Regional wall motion of the left ventricle was evaluated using the centerline method (16,17). The centerline between the end-diastolic and end-systolic contours was generated by computer, and 100 equally spaced chords were drawn perpendicular to the centerline. Coronary artery territories used in the centerline method were chords 51–80 of the RAO projection for the right coronary artery, chords 10–66 of the RAO projection for the left anterior descending coronary artery, and chords 19–67 of the LAO projection for the circumflex coronary artery. Regional wall motion was represented as the average standard deviation above or below the normal mean motion of the chord in 50 normal patients.

Estimation of Infarct Size with Thallium-201 Single Photon Emission Computed Tomography

Resting thallium-201 myocardial scintigrams were obtained approximately 1 month after the onset of AMI. Single-photon emission computed tomography was performed after intravenous injection of thallium-201 of 111 MBq using a large field-of-view single-crystal gamma camera (400 AC, General Electric) interfaced with a computer system (Starcam, General Electric). Thirty-two projections were obtained in the supine position, 25 sec apart, beginning from the 45-degree RAO projection, ro-

tating over 180 degrees to the 45-degree left posterior oblique projection. Images were reconstructed using standard filtered back-projection techniques, with a Butterworth filter (cutoff frequency, 0.4 cycle/cm; power, 10). Tomography was used to quantify the infarct size by creating computer-generated bull's-eye maps of the three dimensional thallium-201 activity in the heart. The bull's-eye maps for each patient were compared with those of 50 normal control subjects from a gender-matched data bank. The pixel count was considered abnormal if it was smaller than -2.5 standard deviations of its corresponding normal mean pixel count. Infarct size was then expressed as the percentage of abnormal pixels in the total bull's-eye map.

Statistical Analysis

Comparisons between the patients with HMI (HMI group) and without HMI (non-HMI group) were made using the Mann-Whitney U test and Fisher's exact probability test. Comparisons between the acute and chronic studies within group were made using a Wilcoxon signed ranks test. Comparisons among signal intensity of various regions were made using ANOVA and Scheffe's F test. Data are expressed as the mean \pm standard deviation. $p < 0.05$ was considered statistically significant.

RESULTS

Autopsy Findings Versus MR Imaging

Intramycardial hemorrhage was visible macroscopically in the subendocardial to midmyocardial layers of the anteroseptal region (Fig. 1A). T1-weighted spin-echo

image showed a homogeneously intense pattern (Fig. 1B), which distinguished intramycardial hemorrhage neither from infarcted nor from distant normal myocardium. In contrast, T2*-weighted gradient-echo image (Fig. 1C) showed a distinct hypointense zone, the location of which coincided with that of the intramycardial hemorrhage present on the pathologic specimen.

Findings in Subjects Without Heart Disease

A homogeneously gray intensity of the myocardium by T2*-gradient-echo imaging was found in all control subjects. The average signal intensity ratio of myocardium and ventricular cavity was 0.69 ± 0.11 and 1.26 ± 0.17 , respectively. There was significant difference between myocardium and ventricular cavity. Thus, the structures of both myocardium and ventricular cavity were clearly identified in T2*-weighted gradient-echo imaging.

These findings confirmed that T2*-weighted gradient echo is capable of imaging intramycardial hemorrhage as a distinct hypointense area and that no false-positive image was found among control subjects.

Studies in Patients with AMI

The T2*-weighted gradient-echo images of 13 of the 39 patients showed distinct hypointense zones in the area at risk, suggesting the presence of intramycardial hemorrhage. In the HMI group, signal intensity ratio of central dark zone of infarction, peripheral region, and remote region were 0.27 ± 0.12 , 0.67 ± 0.17 , and 0.63 ± 0.11 , respectively. In non-HMI, signal intensity ratio of area at risk and remote myocardium were 0.68 ± 0.16 and



Figure 1. (A) Transverse section of the left ventricle with intramycardial hemorrhage visible in the anteroseptal region of the left ventricular myocardium as black areas (white arrowheads). (B) The T1-weighted spin-echo image shows no changes attributable to the intramycardial hemorrhage. (C) T2*-weighted gradient-echo image shows large marked hypointense areas consistent with the histologic evaluation of the hemorrhage (arrowheads).

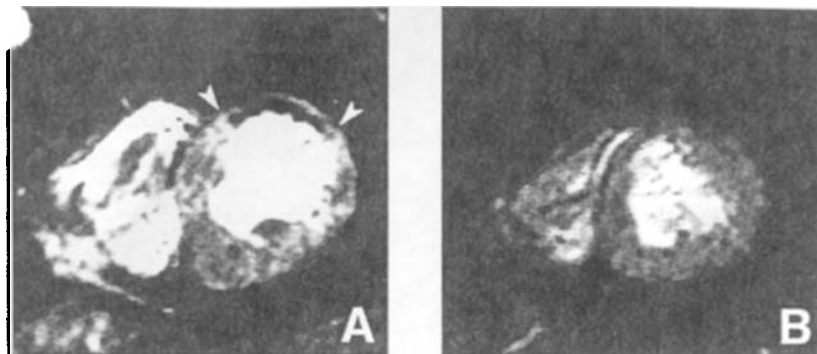


Figure 2. Representative cases of HMI (A) vs. non-HMI (B). ECG-gated T2*-weighted gradient-echo image shows a distinct hypointense zone in the anterior region (white arrowheads), consistent with hemorrhagic myocardial infarction (A). In contrast, the homogeneous intensity of the myocardium in B is consistent with a non-HMI.

0.72 ± 0.13 , respectively. There were no differences in signal intensity ratio among remote normal myocardium, peripheral region of center of infarction, and myocardium of control subjects. Only the central dark zone of infarction showed significantly low signal intensity ($p < 0.05$). Thus, intramyocardial hemorrhage can be detected as a distinct central dark zone in area at risk by T2*-weighted gradient-echo imaging. Representative cases with and without intramyocardial hemorrhage are shown in Fig. 2. The presence of intramyocardial hemorrhage is indicated by a zone of distinct low signal intensity on ECG-gated T2*-weighted gradient-echo image (Fig. 2A). In contrast, no area of decreased signal intensity is visible on the right panel (Fig. 2B). To evaluate the long-term effects of intramyocardial hemorrhage, MRI was repeated approximately 1 month later. In all patients with HMI, the low signal intensity zone in the risk area that

was identified in the acute stage was still visible (Fig. 3). In contrast, patients with non-HMI showed homogeneous signal intensity in the chronic and acute stages.

Patient Characteristics

Table 1 compares some characteristics between patients in the HMI vs. non-HMI groups. There were no age or gender differences between the two groups. Patients in the HMI group had higher incidence of electrocardiographic Q wave than in the non-HMI group (92% vs. 46%, $p < 0.05$). Congestive heart failure tended to be more prevalent in the HMI group ($p = 0.45$). Patients with anterior infarctions had a higher incidence of HMI than patients with inferior or posterior infarctions (52% vs. 11%, $p < 0.05$).

The coronary angiographic findings are shown in

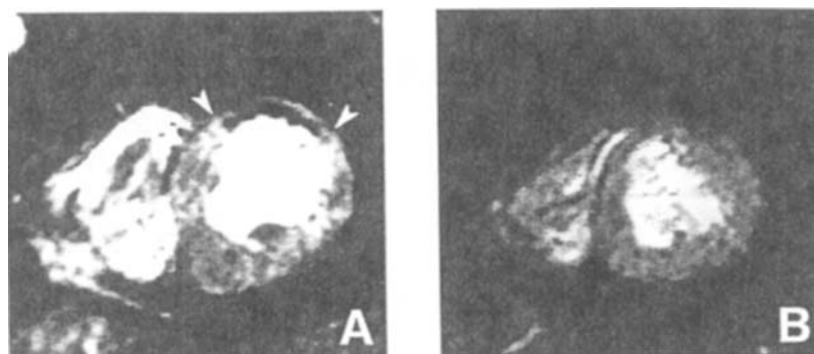


Figure 3. Representative magnetic resonance images of the left ventricular short-axis plane of a patient with inferior HMI in the acute stage (A) and in the chronic stage (B). Gradient-echo image 5 days after coronary reperfusion shows the existence of intramyocardial hemorrhage as a marked hypointense zone in the inferior region (white arrows). There is still a hypointense zone in the same region 28 days after coronary reperfusion (white arrows).

Table 1
Patient Characteristics With and Without Intramyocardial Hemorrhage

	HMI (n = 13)	Non-HMI (n = 26)	p
Age (yr)	63 ± 9	63 ± 11	0.96
Gender (male/female)	7/6	17/9	0.51
ECG Q wave, n (%)	12 (92)	12 (46)	0.01
Congestive heart failure, n (%)	5 (38)	6 (23)	0.45
Culprit vessels			
LAD	11	10	
RCA	1	13	
LCX	1	3	

LAD, left anterior descending coronary artery; LCX, left circumflex coronary artery; RCA, right coronary artery.

Table 2. The average TIMI flow grade was slightly lower in the HMI group than in the non-HMI group. Collateral flow grade was estimated in the 30 patients with TIMI flow grade 0 or 1. Average collateral flow grade was not significantly different between the two groups (1.1 ± 0.9 in the HMI group vs. 1.2 ± 0.7 in the non-HMI group). However, the HMI group included a significantly higher number of patients with poor collateral flow than the non-HMI group (81% vs. 37%, $p = 0.03$). Because the interval between onset of infarction and reperfusion could not be estimated in the patients with spontaneous reperfusion (TIMI flow grades 2 and 3), it was assessed only in the 30 patients with TIMI flow grades of 0 and 1. The interval from onset of infarction to reperfusion tended to be longer in the HMI group than in the non-HMI group ($p = 0.37$). There was no difference in the incidence of intra-

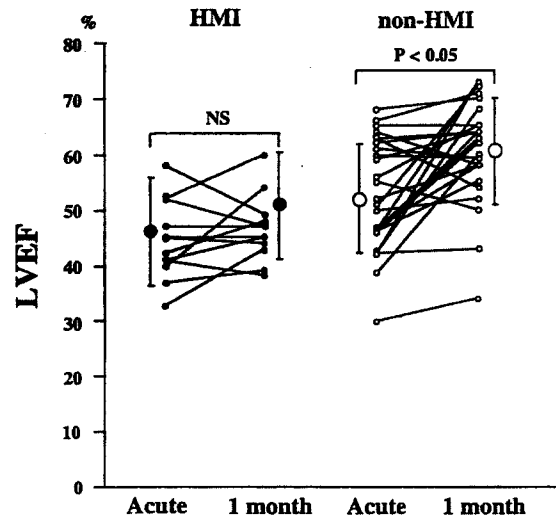


Figure 4. Left ventricular ejection fraction (LVEF) in the acute phase and 1 month after AMI. ●, patients with HMI; ○, patients without HMI (non-HMI). There was significant recovery of left ventricular ejection fraction in the non-HMI group but not in the HMI group.

myocardial hemorrhage between early reperfusion and late reperfusion ($p = 0.69$).

Left Ventricular Functional Outcome

The global left ventricular ejection fraction did not increase in the HMI group ($47 \pm 9\%$ to $51 \pm 10\%$), whereas that in the non-HMI group increased from $53 \pm 10\%$ to $60 \pm 9\%$ 1 month later ($p < 0.05$), as shown in Fig. 4.

Table 2
Coronary Angiographic Findings in the Acute Phase

	HMI (n = 13)	Non-HMI (n = 26)	p
TIMI flow grade	0.4 ± 0.8	0.7 ± 1.1	0.38
0	10	17	
1	1	2	
2	2	4	
3	0	3	
Collateral flow	n = 11	n = 19	
Good/poor	2/9	12/7	0.03
Time to reperfusion (hr)	10.3 ± 13.9	7.1 ± 5.9	0.37
Early reperfusion (≤ 6 hr), n (%)	6 (32)	13 (68)	0.69
Late reperfusion (> 6 hr), n (%)	5 (45)	6 (55)	

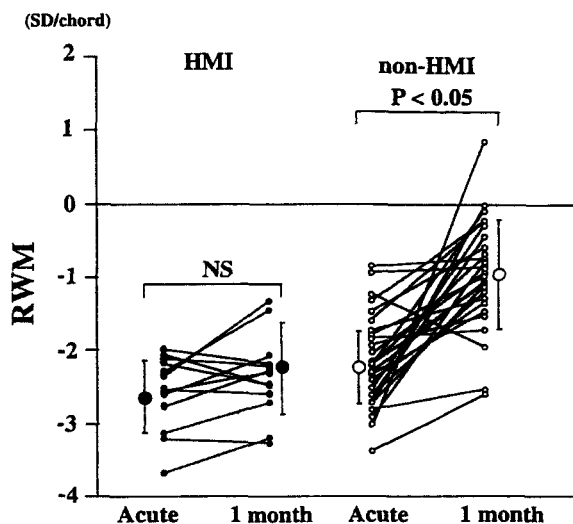


Figure 5. Regional wall motion (RWM) in the risk area, using the centerline method at the acute and chronic stages. ●, patients with HMI; ○, patients without HMI (non-HMI). There was significant improvement in RWM in the non-HMI group, but no improvement was found in the HMI group.

Regional wall motion within the risk area in both groups is shown in Fig. 5. There was no difference between the two groups in the acute stage (-2.63 ± 0.48 in the HMI group vs. -2.23 ± 0.52 SD/chord in the non-HMI group). However, there was a significant difference between the two groups at 1 month (-2.23 ± 0.61 for the HMI group vs. -0.98 ± 0.77 for the non-HMI group, $p < 0.05$). Thus, neither global nor regional wall motion improved in the HMI group, whereas both parameters

showed improvement in the non-HMI group 1 month later ($p < 0.05$).

Estimated Infarct Size

Infarct size, estimated from peak serum CK levels and thallium-201 scintigraphy, is shown in Fig. 6. The HMI group had higher peak serum CK levels and larger infarct sizes than the non-HMI group ($3,862 \pm 1,825$ IU/l vs. $1,575 \pm 818$ IU/l for peak CK, $p < 0.01$; $37 \pm 13\%$ vs. $20 \pm 21\%$ for infarct size, $p < 0.01$).

DISCUSSION

In the present study, intramyocardial hemorrhage was clearly visible, on ECG-gated T2*-weighted gradient-echo MR images, as a distinct hypointense zone in the area at risk. A comparison of pathologic findings and MR images in an autopsy case enabled us to validate the detection of intramyocardial hemorrhage by T2*-weighted gradient-echo MR imaging. This study demonstrates that MR imaging can detect the presence of intramyocardial hemorrhage in patients with reperfused AMI and that HMI is unexpectedly common in patients with nonfatal AMI. Although MR imaging has been used to image myocardial infarctions in humans (18–21), there are no published clinical studies of its use in the detection of intramyocardial hemorrhage. Only Johnston et al. (21) have speculated, in their study with T2-weighted spin-echo MR imaging, that heterogeneous images may be partly due to intramyocardial hemorrhage.

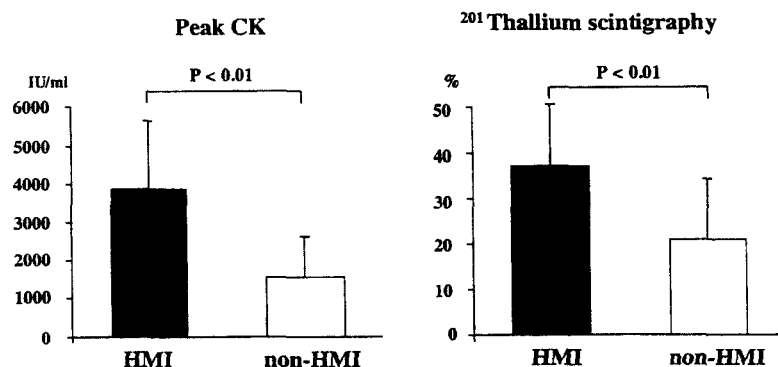


Figure 6. Infarct size estimated by peak serum CK levels and thallium-201 scintigraphy. Both measurements are consistent with a significantly larger infarct size in the HMI group than in the non-HMI group.

Methodological Considerations

The detection of intracranial hemorrhage by MR imaging, based on paramagnetic effect of blood breakdown products, has been reported in detail by several investigators (7–11). Hemoglobin in hemorrhagic tissue breaks down into several hemoglobin metabolites (oxyhemoglobin, deoxyhemoglobin, and methemoglobin) and finally to ferritin and hemosiderin. These blood degradation products are paramagnetic substances causing local magnetic field inhomogeneities, which result in distinct hypointensity in susceptibility-weighted MR imaging (22). In an earlier experimental study, *ex vivo* T2-weighted spin-echo imaging was used to detect intramyocardial hemorrhage (13). However, T2*-weighted gradient-echo MR imaging was used in this study for two reasons: its high sensitivity for magnetic susceptibility effects and its shorter acquisition time compared with ECG-gated T2-weighted spin-echo imaging. In clinical settings, a shorter acquisition time is an advantage, especially when the patient is in the midst of an AMI.

Although we demonstrated that hypointensity area in T2*-weighted gradient-echo imaging coincided with an area of intramyocardial hemorrhage in an autopsy case, it may be questioned whether the hypointensity zone by T2*-gradient-echo imaging in the myocardium at risk truly represents the intramyocardial hemorrhage itself. It is unlikely that the other substances or tissue changes cause inhomogeneities of the magnetic field, such as fibrosis or calcific lesions, except for intramyocardial hemorrhage in reperfused AMI, because all patients in this study had first AMI with single-vessel disease and no possibility of other heart diseases.

The degree of sensitivity and specificity of *in vivo* imaging in the detection of intramyocardial hemorrhage remains unclear. However, the gradient-echo sequence used in the present study can be sensitive to magnetic susceptibility. Furthermore, when performing cardiac MRI, we used a high magnetic field apparatus (1.5 T), which detects the magnetic susceptibility products more effectively. Therefore, we believe that this technique has high sensitivity to detect intramyocardial hemorrhage in clinical settings.

When Should MRI Be Performed?

Intramyocardial hemorrhage and infarct tissue are gradually absorbed and replaced by fibrosis over time. However, the effects of intramyocardial hemorrhage on MR images in the long term are unclear. Although an experimental study found that the healing process was more rapid in the reperfused myocardium than in the non-

reperfused myocardium (23), intramyocardial hemorrhage in a human autopsy study by Mathey et al. (1) was found as late as day 18 after the onset of AMI, suggesting a delay in the healing process of hemorrhage. In the present study, intramyocardial hemorrhage was visible as a low signal intensity zone even 1 month after coronary reperfusion. This finding suggests that absorption of an intramyocardial hemorrhage may take a long time in humans. MR examination from 2 to 14 days after coronary reperfusion may be reliable for detecting intramyocardial hemorrhage.

In the early acute period, intramyocardial hemorrhage detection is limited. In the intracranial hemorrhage study, a hemorrhage that is less than 12 hr old cannot be distinguished from other edematous masses in MR images (9). This can be explained by the facts that it takes several hours for oxyhemoglobin to be transformed into deoxyhemoglobin and that intramyocardial hemorrhage itself takes several hours to develop after thrombolysis (4). Therefore, in the present study, MRI was performed at least 24 hr after PTCA.

Clinical Implications of HMI

With the advent of thrombolytic therapy, an increasing prevalence of intramyocardial hemorrhage has been reported (1–6). However, its true prevalence and clinical significance remain unknown because of the absence of an established clinical method to detect it. Previous reports of HMI in humans are based on autopsy studies, and HMI has been rare in fatal AMI without coronary recanalization. Among patients who died of AMI without thrombolytic therapy, Mathey et al. (1) found no HMI in a review of 195 cases, Waller (24) found three of 119 patients (2%), and Fujiwara et al. (4) reported 2 of 60 patients (3%). In contrast, the incidence of HMI in fatal AMI treated with thrombolytic therapy is much higher. Fujiwara et al. (4) described intramyocardial hemorrhages in 15 of 18 (83%) and Mathey et al. (1) in 4 of 6 cases (66%), whereas Waller et al. (5) found 14 cases of HMI in 19 patients (74%). On the basis of these observations, most clinicians believe that recanalization of the infarct-related artery is the main cause of HMI. The prevalence of HMI in our study (33%) was lower, probably because, unlike our patients, those included in these previous reports had sustained fatal AMI.

A possible determinant of HMI may be the infarct size. In the present study, the HMI group had significantly larger infarct sizes than the non-HMI group. In addition, they had significantly less anterograde and collateral flow. These findings suggest that large infarct size and poor development of collateral flow are closely asso-

ciated with the occurrence of intramyocardial hemorrhage. In reperfused animal models, the severity of HMI is associated with the duration of coronary artery occlusion (25) and poor development of collateral flow (26). Both factors are also the major determinants of infarct size in humans (27–29). Our previous study strongly suggests that intramyocardial hemorrhage detected by MR imaging is closely related to the microvascular damage assessed by myocardial contrast echocardiography in patients with reperfused AMI (14). Restoration of blood flow to the areas where microvascular injury has taken place results in intramyocardial hemorrhage because of damage of both myocardial cells and microcirculation. The poor recovery of left ventricular function in the HMI group may be due to the consequence of irreversible myocardial injury rather than the intramyocardial hemorrhage. However, whether or not intramyocardial hemorrhage after coronary reperfusion has an adverse effect on the recovery of left ventricular function and whether or not reperfusion, by PTCA alone or by thrombolytics, modifies the incidence of HMI in human remains to be investigated.

CONCLUSIONS

The present study demonstrates the potential usefulness of ECG-gated T2*-weighted gradient-echo MR imaging in the detection of intramyocardial hemorrhage, which appears as a zone of decreased signal intensity. HMI was observed in nearly one third of patients undergoing primary PTCA and was more frequently found in large zones of irreversibly injured myocardium.

REFERENCES

1. Mathey DG, Schofer H, Kuck KH, Beil U and Kloeppel G. Transmural, haemorrhagic myocardial infarction after intracoronary streptokinase. Clinical, angiographic, and necropsy findings. *Br Heart J*, 1982; 48:546–551.
2. Kao KJ, Hackel DB and Kong Y. Hemorrhagic myocardial infarction after streptokinase treatment for acute coronary thrombosis. *Arch Pathol Lab Med*, 1984; 108:121–124.
3. Topol EJ, Herskowitz A and Hutchins GM. Massive hemorrhagic myocardial infarction after coronary thrombolysis. *Am J Med*, 1986; 81:339–343.
4. Fujiwara H, Onodera T, Tanaka M, Fujiwara T, Wu DJ, Kawai C and Hamashima Y. A clinicopathological study of patients with hemorrhagic myocardial infarction treated with selective coronary thrombolysis with urokinase. *Circulation*, 1986; 73:749–757.
5. Waller BF, Rothbaum DA, Pinkerton CA, Cowley MJ, Linnermeier TJ, Orr C, Irons M, Helmuth RA, Wills ER and Aust C. Status of the myocardium and infarct-related coronary artery in 19 necropsy patients with acute recanalization using pharmacologic (streptokinase, r-tissue plasminogen activator), mechanical (percutaneous transluminal coronary angioplasty) or combined type of reperfusion therapy. *J Am Coll Cardiol*, 1987; 9:785–801.
6. Gertz SD, Kalan JM, Kragel AH, Roberts WC, Braunwald E and TIMI Investigators. Cardiac morphologic findings in patients with acute myocardial infarction treated with recombinant tissue plasminogen activator. *Am J Cardiol*, 1990; 65:953–961.
7. Gomori JM, Grossman RI, Goldberg HI, Zimmerman RA and Bilniuk LT. Intracranial hematomas: imaging by high-field MR. *Radiology*, 1985; 157:87–93.
8. Atlas SW, Mark AS, Grossman RI and Gomori JM. Intracranial hemorrhage: gradient-echo MR imaging at 1.5T. *Radiology*, 1988; 168:803–807.
9. Seidenwurm D, Meng TK, Kowalski H, Weinreb JC and Kricheff II. Intracranial hemorrhagic lesions: Evaluation with spin-echo and gradient-refocused MR imaging at 0.5 and 1.5 T. *Radiology*, 1989; 172:189–194.
10. Greenberg SM, Finklestein SP and Schaefer PW. Petechial hemorrhages accompanying lobar hemorrhage: Detection by gradient-echo MRI. *Neurology*, 1996; 46:1751–1754.
11. Patel MR, Edelman RR and Warach S. Detection of hyperacute primary intraparenchymal hemorrhage by magnetic resonance imaging. *Stroke*, 1996; 27:2321–2324.
12. Lotan CS, Miller SK, Cranney GB, Pöhost GM and Elgavish GA. The effect of postinfarction intramyocardial hemorrhage on transverse relaxation time. *Magn Res Med*, 1990; 23:346–355.
13. Lotan CS, Bouchard A, Cranney GB, Bishop SP and Pöhost GM. Assessment of postreperfusion myocardial hemorrhage using proton NMR imaging at 1.5 T. *Circulation*, 1992; 86:1018–1025.
14. Asanuma T, Tanabe K, Ochiai K, Yoshitomi H, Nakamura K, Murakami Y, Sano K, Shimada T, Murakami R, Morioka S and Beppu S. Relationship between progressive microvascular damage and intramyocardial hemorrhage in patients with reperfused anterior myocardial infarction. *Circulation*, 1997; 96:448–453.
15. Rentrop KP, Cohen M, Blanke H and Phillips RA. Changes in collateral channel filling immediately after controlled coronary artery occlusion by an angioplasty balloon in human subject. *J Am Coll Cardiol*, 1985; 5:587–592.
16. Sheehan FH, Bolson EL, Dodge HT, Mathey DG, Schofer J, Woo HW. Advantage and applications of the centerline method for characterizing regional ventricular function. *Circulation*, 1986; 74:293–305.
17. Sheehan FH, Schofer J, Mathey DG, Kellett MA, Smith H, Bolson EL and Dodge HT. Measurement of regional

- wall motion from biplane contrast ventriculograms: a comparison of the 30 degree right anterior oblique and 60 degree left anterior oblique projections in patients with acute myocardial infarction. *Circulation*, 1986; 74:796-804.
18. Yokota C, Nonogi H, Miyazaki S, Goto Y, Maeno M, Daikoku S, Itho A, Haze K and Yamada N. Gadolinium-enhanced magnetic resonance imaging in acute myocardial infarction. *Am J Cardiol*, 1995; 75:577-581.
 19. McNamara MT, Higgins CB, Schechtman N, Botvinick E, Lipton M, Chatterjee K and Amparo EG. Detection and characterization of acute myocardial infarction in man with use of gated magnetic resonance. *Circulation*, 1985; 71:717-724.
 20. de Roos A, van Rossum AC, van der Wall E, Postema S, Doornbos J, Matheijssen N, van Dijkman PR, Visser FC and van Voorthuisen AE. Reperfused and nonreperfused myocardial infarction: Diagnostic potential of Gd-DTPA-enhanced MR imaging. *Radiology*, 1989; 172:717-720.
 21. Johnston DL, Wendt RE, Mulvagh SL and Rubin H. Characterization of acute myocardial infarction by magnetic resonance imaging. *Am J Cardiol*, 1992; 69:1291-1295.
 22. Bradley WG. MR appearance of hemorrhage in brain. *Radiology*, 1993; 189:15-26.
 23. Roberts CS, Schoen FJ and Kloner RA. Effect of coronary reperfusion on myocardial hemorrhage and infarct healing. *Am J Cardiol*, 1983; 52:610-614.
 24. Waller BF. Pathology of new investigation in the treatment of coronary heart disease. *Curr Probl Cardiol*, 1986; 11:666-760.
 25. Garcia-Dorado D, Theroux P, Solares J, Alonso J, Fernandez-Aviles F, Elizaga J, Soriano J, Botas J and Munoz R. Determinants of hemorrhagic infarcts: histologic observations from experiments involving coronary occlusion, coronary reperfusion, and reocclusion. *Am J Pathol*, 1990; 137:301-311.
 26. Higginson LA, White F, Heggveit HA, Sanders TM, Bloor CM and Covell JW. Determinants of myocardial hemorrhage after coronary reperfusion in the anesthetized dog. *Circulation*, 1982; 65:62-69.
 27. Clements IP, Christian TF, Higano ST, Gibbons RJ and Gersh BJ. Residual flow to the infarct zone as a determinant of infarct size after direct angioplasty. *Circulation*, 1993; 88:1527-1533.
 28. Habib GB, Heibig J, Forman SA, Brown BG, Roberts R, Terrin ML, Bolli R, and TIMI Investigators. Influence of coronary collateral vessels on myocardial infarct size in humans: results of phase I thrombolysis in myocardial infarction (TIMI) trial. *Circulation*, 1991; 83:739-746.
 29. Christian TF, Schwartz RS and Gibbons RJ. Determinants of infarct size in reperfusion therapy for acute myocardial infarction. *Circulation*, 1992; 86:81-90.